JOURNAL OF MATERIALS SCIENCE 26 (1991) 1882–1890

Thermal, mechanical and chemical effects in the degradation of the plasma-deposited α-SiC:H passivation layer in a multilayer thin-film device

L. S. CHANG, P. L. GENDLER, J.-H. JOU*
IBM Research Division, Almaden Research Center, 650 Harry Road, San Jose, California 95120-6099, USA

Amorphous, hydrogenated silicon carbide (α-SiC:H) deposited by a plasma-enhanced-chemical-vapour-deposition (PECVD) process has been used as the topmost passivation layer in a multilayer thin-film device, namely, a thermal ink-jet printhead. Normal operations of the device involve rapid heating of the multilayer structure at several kHz, repetitively forming vapour bubbles that grow and collapse in an otherwise liquid environment. During such operations, the α-SiC:H layer is subjected to a variety of thermal, mechanical and chemical stresses that are detrimental to its integrity. It is found that thermally activated failures may occur when the multilayer structure is driven for extended periods of time or by pulses of excessive magnitude or duration, or when the α-SiC:H film is so thick as to store excessive elastic energy due to large differential thermal expansion effects. It is also found that severe mechanical (namely, cavitation) effects associated with bubble collapse cause early device failures if the surface of the device is exposed to an unlimited liquid reservoir; however, such adverse effects are greatly mitigated by the presence of a nozzle plate in the vicinity of the top surface. Finally, it is shown that high pH and various chemicals tend to etch the α-SiC:H thin film through an oxidation-dissolution process, removing the passivating material rapidly and leading to device failures.

1. Introduction

Silicon carbide, in view of its excellent wear and corrosion resistance as well as thermal stability, has been prepared by several processes to provide surface coatings in a variety of applications [1–5]. Specifically, plasma-assisted depositions, such as the plasma-enhanced chemical vapour deposition (PECVD), have been used to produce films at low substrate temperatures (250–500 °C) [6–10]. Silicon carbide films made by a PECVD process are quite different from conventional SiC films in that the former are amorphous, hydrogenated, and have varying compositions depending upon equipment design, deposition conditions, gas flow rates, etc. They are, in effect, a different class of materials from stoichiometric, crystalline SiC, and are better represented by α-Si_xC_{1-x}:H, where the hydrogen is weakly bonded in these metastable films, evolving near and above the deposition temperature. Recently, α-Si_xC_{1-x}:H as well as other variant thin films have been used as the encapsulating material for the final passivation of semiconductor and electronic devices, and are shown to have various superior properties [11–14]. However, few articles have been published on the breakdown of such overcoats under specific operating conditions. In this context, various thermal, mechanical and chemical effects in the degradation of the α-SiC:H ($x \approx 0.5$) passivation layer deposited on top of a thermal ink-jet device are herein reported.

Because of lower manufacturing costs associated with planar thin-film technology and easy adaptability to both high and low end printing applications, thermal ink-jet has recently become the technology of choice for drop-on-demand ink-jet printing [15–17]. A schematic representation of a typical thermal ink-jet device as well as its working mechanism is included as Fig. 1. A thin resistive film is rapidly heated through a joule-heating process by direct-current (d.c.) electrical pulses which pass through the resistor and each time last a few microseconds. The temperature at the top surface of the device is raised, instantaneously, to over 300 °C at the end of each pulse, forming, mainly through homogeneous nucleation, a blanket of vapour bubble in the ink over the surface of the device. The rapid growth and collapse of the bubble causes an ink drop to be ejected from a nearby orifice or nozzle. A printhead contains arrays of such miniature heaters, each operated at several kHz, and is therefore capable

*Currently with the Materials Science and Engineering Department, National Tsing-Hua University, Hsinchu 30043, Taiwan.

0022–2461/91 $03.00 + .12

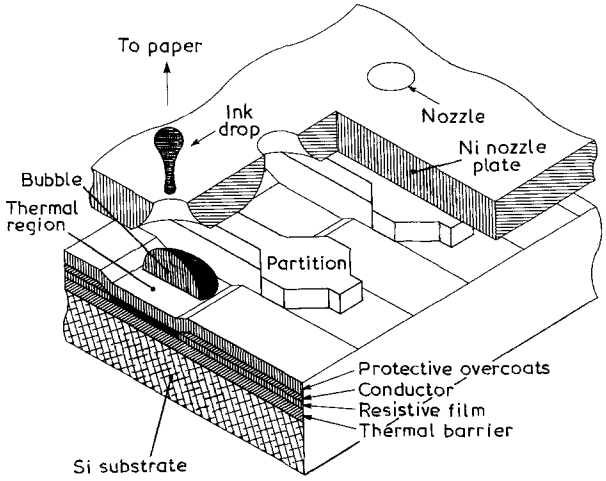

Figure 1 A schematic showing a typical thermal ink-jet device and its working mechanism. The top protective overcoat is usually composed of α-SiC:H.

of high-speed printing. The ink may be either solvent or aqueous based, may contain, in addition to dyes, a variety of ingredients such as electrolytes, surface-active agents, polymers, biocides, etc., and may have an acidic or basic pH value. Thus, during storage and operation the ink-jet device is subjected to several thermal, mechanical and chemical influences which may be deleterious to the performance and lifetime of the device [18, 19]. Since α-SiC:H films are often used as the top overcoat [16, 17], the issues of device lifetime and performance are ultimately determined by the degradation of α-SiC:H under these stressful influences.

In the present study, several major problematic causes in the breakdown of thermal ink-jet printheads are discussed, including thermal stress, cavitation-induced damage, and chemical etching due to various ink components. Attention is focused upon the material aspects of the carbide top overcoat under these conditions.

2. Experimental details

2.1. Materials

The choice of materials for a thermal ink-jet device has been discussed previously [16–19]. Briefly, the substrate consists of silicon, though alumina or glass can also be used, on top of which is a thermal barrier layer, normally a thermally grown silicon dioxide layer. Over this a thin film of resistive material such as HfB_2, Ta_2Al or TaN is sputter-deposited and photolithographically patterned, followed by the deposition and patterning of a conducting material, normally Al-Cu or Au. The conductor and resistor layers are then protected by two overcoat layers, usually a PECVD α-SiN:H layer and a PECVD α-SiC:H layer, each 200–500 nm thick. Other materials such as sputtered silicon oxide, tantalum or zirconium can also be used. Occasionally, a polyimide coating over the conductors away from the thermal region is laid down for extra protection. Finally, a nozzle plate with designed geometries, normally made of electroformed nickel, is bonded to the photoresist to form ink channels. Partitions between adjacent channels are made of either nickel or photoresist.

In the present study, the top overcoat of the device is a PECVD silicon carbide film. Described in detail elsewhere [14], the films are deposited in tubular or parallel-plate reactors at 350–450 °C, thus without affecting metallization underneath. The reactor is operated at a pressure of 266.6 Pa or less; entrant gases are methane and silane, often diluted in argon. The average thickness of the film is about 300 nm.

The solvent for the various chemicals examined is either deionized water or aqueous solutions of diethylene or ethylene glycol. The concentration of glycol varies from 15 to 50%. All chemicals, except dyes, are analytical grade.

2.2. Test procedures

The printhead is filled with the test solution and mounted such that vapour bubbles or streams of drops for each individual channel can be monitored by a video camera illuminated by a synchronized strobe-light source. The individual heaters are driven by 3–6 μs d.c. pulses at various voltages and frequencies. A typical device has a resistance between 65 and 70 ohms and is normally driven by 19 to 20 V. The minimum voltage required for stable nucleation and drop ejection is around 16.5 V, which drives surface temperature to just over 300 °C. After testing for specific periods of time, the printhead is disassembled. The device surface is gently rinsed with deionized water before inspection and characterization.

In the study of mechanical (i.e. cavitation) damages, two kinds of test environment were employed. The open-pool testing consists of driving the heaters while the latter are immersed in a pool of the test liquid; typical dimensions of the test geometry were arranged such that the liquid pool can be regarded as an infinite reservoir for the device, from the viewpoint of both momentum and heat transport [18, 19]. In closed-pool tests the nozzle plate of the device is left intact while the test liquid is supplied continuously to the individual ink channels during operation. In a third group of experiments, a transparent plate is placed in parallel to the heater surface at a known distance. Closed-pool tests only are performed in the study of thermal and chemical effects.

2.3. Sample characterization

The compositions and microstructures of the α-SiC:H thin films are studied by a variety of methods, including Scanning electron microscopy (SEM), Rutherford backscattering spectrometry (RBS), Scanning auger microscopy (SAM), Electron probe micro-analysis (EPMA), and energy-dispersive X-ray analysis (EDX). A gold–palladium thin film is sputter-deposited on the sample surface before examination if sample charging is present. The surface topography of specimens before and after testing is determined by the contact profile method, depicted in Fig. 2. Being a non-destructive method, this technique is easy to apply and generates reproducible readings in most instances.

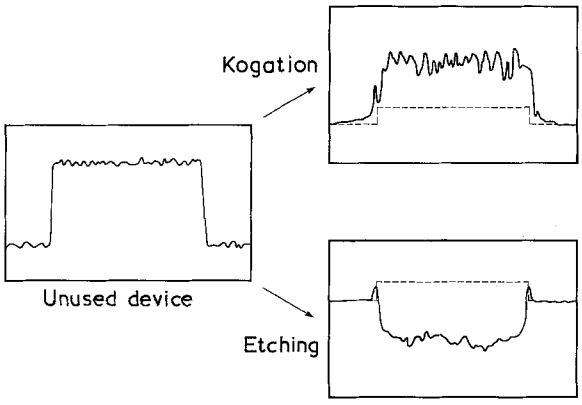

Figure 2 Surface profiles of three typical devices as determined by contact profilometry.

3. Results and discussion

Based on results of RBS and related forward scattering techniques, the compositions of the typical α-SiC:H thin film used in the present study in terms of atomic percentages are; Si: 35 ± 2%; C: 35 ± 4%; H: 25 ± 4%; other elements (O and N), less than 5%. Since the Si/C ratio is close to unity, the microstructure of the film can be described as follows: (1) the film is composed of myriads of partially cross-linked, C and H substituted polysilicon backbones [20]; (2) the film contains sp^3 and sp^2 carbons and has both clusters of hydrogen atoms and regions devoid of hydrogen [21].

3.1. Effects of thermal stresses

Miscellaneous origins and mechanisms may give rise to stress and strain in thin film structures. As a matter of definition, the total stress in the structure is made up of two terms, i.e., stress due to differential thermal expansion effects and that due to all other contributions, such as stress due to argon incorporation, impurities, microvoids, dislocations, etc. (namely, intrinsic stress) [22]. The thermal expansion mismatch effects are generally amenable to calculation, provided thermal properties of the films and the substrate are available. The present structure, in its operation mode, is thermally cycled between room temperature and 300-plus °C, at repetition rates of several kHz. In this respect, thermal stress in each layer due to thermal expansion mismatch is calculated. While details are described elsewhere [23], an example is given in Fig. 3, showing that stresses in the carbide layer and the resistor due to thermal expansion mismatch with adjacent layers may approach 1 GPa under normal operating conditions. Because of the relatively small thermal expansion coefficient of Si ⟨1 0 0⟩, such stresses are compressive in nature as the device temperature increases. Another example is shown in Fig. 4, where the instantaneous elastic energy stored in the carbide layer at its peak temperature is plotted against thickness of the layer. Since there is a limit to the amount of energy a thin film can store without exceeding the critical energy for film fracture and delamination [24, 25], a carbide film having a thickness of 1.5 μm or more will tend to fracture and delaminate,

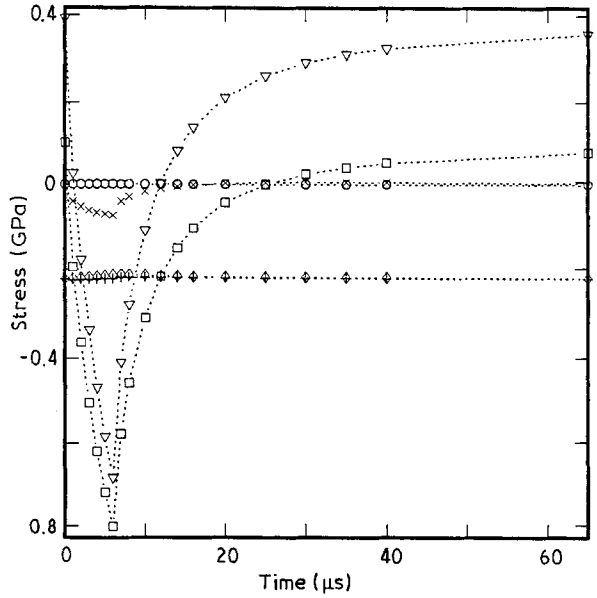

Figure 3 Stresses due to thermal expansion mismatch as a function of time in a thermal cycle. The largest compressive stress in each layer occurs at 6 μs, when the resistor film reaches a peak temperature of 397 °C; (□) carbide overcoat; (×) nitride overcoat, (▽) resistor; (+) thermal barrier; (○) substrate; (◇) substrate backside.

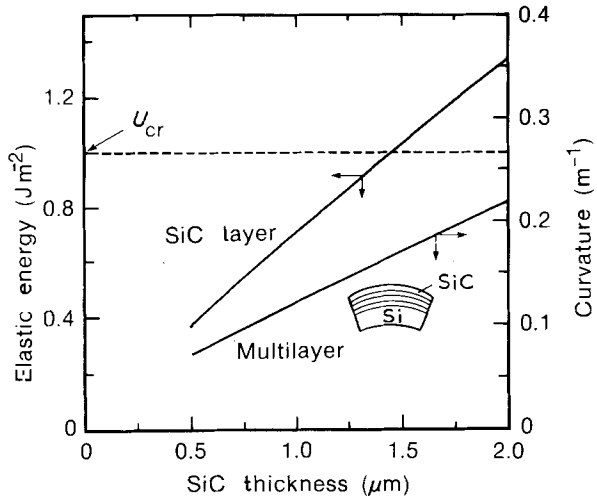

Figure 4 Peak elastic energy and curvature of a silicon carbide film in a multilayer device as a function of film thickness. U_{cr} is the critical energy for adhesion in carbide [24].

even though the film is heated only momentarily in a repetitive manner. Hence, it is not practical to increase the thickness of the carbide film indefinitely so as to enhance its ability to withstand chemical etching (see below).

Although the effect of intrinsic stress is not studied specifically in the present work, it is safe to state that film stress as a whole is primarily responsible for two types of thin film failures, namely, thermal overload and thermal fatigue.

The failure mode of thermal overload, an example of which is shown in Fig. 5b, is independent of the test environment and occurs rapidly when a device is overdriven by pulses of excessive amplitude, duration or frequency. It is characterized by delamination and/or removal of a large, approximately circular area of the carbide–nitride overcoat and the underlying res-

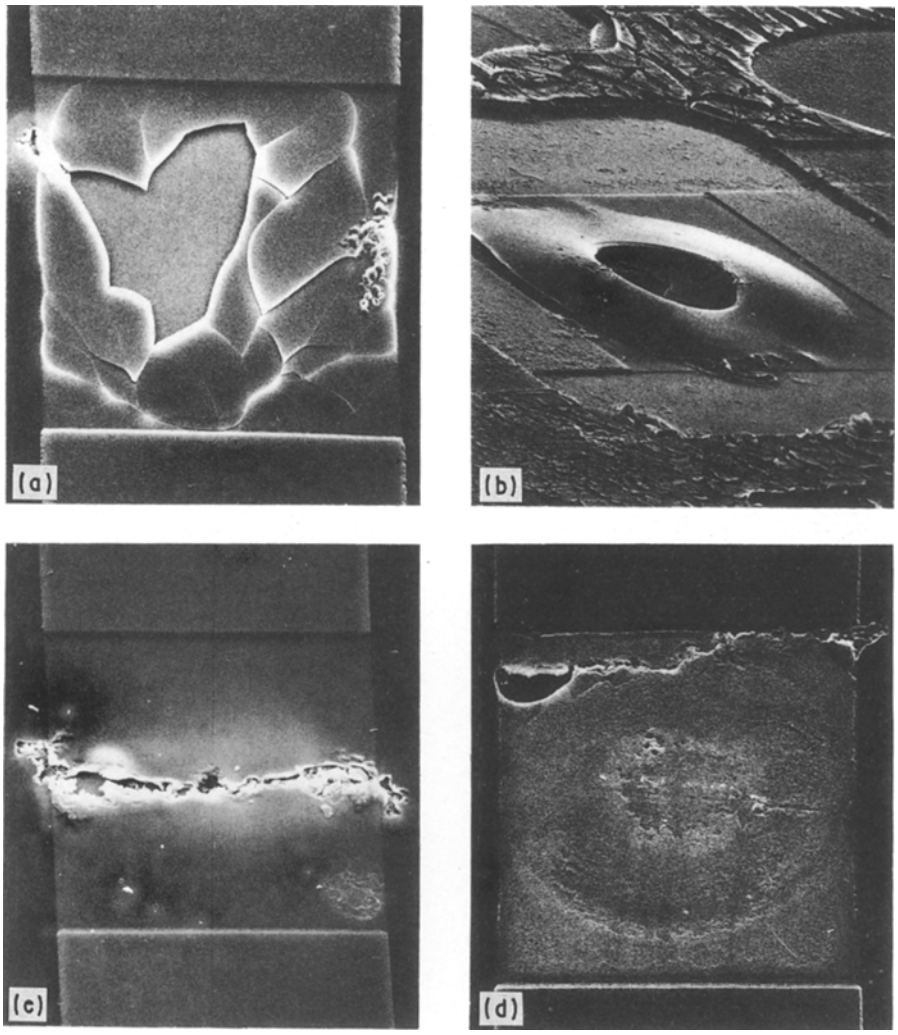

Figure 5 Typical device failure modes; (a) fatigue cracks and delamination; (b) delamination due to thermal overload; (c) cavitation-induced damage; (d) chemical etching of overcoat (kogation layer removed).

istor film, exposing the oxide barrier layer, which is part of the substrate. The composition of each region in a *post-mortem* sample is verified by either EDX or EPMA. The failure mechanism may be as follows: A relatively uniform, huge thermal load is suddenly imposed upon the thin-film structure, causing large thermal expansion misfits among various films; the largest thermal stresses probably exist in the carbide film and the resistor, as explained above. As a result, delamination takes place between the substrate and the resistor. This separation, in turn, disrupts heat dissipation through the substrate, further elevating the temperature in the thin films. It is known that hydrogen atoms in PECVD α-SiC:H and SiN:H films migrate to activation sites and form molecular hydrogen gas when the film temperature is raised above its deposition temperature [14]. Thus, a substantial amount of H_2 gas may be released instantaneously and create a significant internal pressure. Consequently, part or all of the layers are blown off, and the resistor becomes an open circuit.

Another detrimental effect of thermal stresses associated with repeated thermal cycling is fatigue of the thin-film device. This mode of failure often occurs when devices are driven in dry air or an inert gas environment for extended periods, or at greater than normal voltage, frequency or pulse duration. In some of the latter cases the ink used in the test seems to accelerate the fatigue failure, suggesting a corrosion fatigue mechanism. Fig. 5a shows a device failure due to thermal fatigue after prolonged testing in room air; widespread fracture and delamination of the overcoat typify this failure mode.

There is at least one more place where film stress plays a significant role. As will be shown below, most devices tested in a normal operating mode become an open circuit because of a transverse crack across the device near one of the conductor pads. The reason for this proximity is possibly because stress concentrations exist near the step coverages in the sputtered and PECVD thin films.

3.2. Cavitation-induced damages

Under open-pool test conditions, most types of ink-jet thin-film devices appear to have a wide distribution of lifetime. The median or average open-pool lifetime is at least one order of magnitude smaller than its closed-pool counterpart, as is exemplified by Table 1.

TABLE I Typical median heater lifetimes (megacycles)

Fluid medium[a]	Open-pool	Closed-pool
Deionized water	43	–
10% EG	8.5	> 600
30% EG	2.3	–
50% EG	1.8	> 400
50% EG2	2.7	86
Ink A	1.8	> 1500
Ink B	11	> 400

[a] EG is ethylene glycol; EG2 is diethylene glycol.

In virtually all the cases where the device failed after repeated vapour nucleation and bubble growth in an open pool, there is a transverse crack across the central region of the device. The direction of the crack is approximately perpendicular to the direction of the conductor pads; see Fig. 5c. Furthermore, a closer look at the device surface often reveals the presence of craters over the device surface. Several characteristics of the craters include: (1) Most craters appear near the centre of the crack, which often coincides with the geometrical centre of the device; (2) shortly before the device becomes open circuit as a consequence of the transverse crack, a deep centre hole is often formed, presumably by repeated action from the damaging forces; (3) the craters increase in number as a function of test time; (4) under higher magnifications, the boundary of a crater appears to coincide with grain boundaries of several adjacent columns in the α-SiC:H film [18].

A plausible explanation for the above observations is that the craters are mainly generated by the mechanical action of impinging shock wave and/or liquid microjet associated with the collapse of vapour bubbles [26]. Thus, mechanical forces, assisted by local chemical and electrochemical attack, preferentially remove material from those presumably more soluble, intergranular regions of the amorphous overcoat film, leaving holes or craters in the film. Many of the craters, especially the ones near the centre of the device, will appear to grow in size and depth, as mechanical forces are repetitively directed toward them while further chemical actions take place. Strobed video-microscopic observations verify that vapour bubbles almost exclusively collapse near the geometrical centre of the device. Since it is difficult to establish a clear demarcation between mechanical action and the concurrent erosion/corrosion effects, it is adequate to use the term cavitation-induced damage in a generic sense to describe this mode of overcoat failure in a thermal ink-jet device. It must be noted that if a corrosive liquid media is used in the test, the SiC:H film will be damaged at a faster pace [18, 19]. Since the present work is focused upon failure of the SiC:H film, the detailed device failure mechanism subsequent to the overcoat failure is not given here.

The above cavitation-induced damage is unique to the three-phase (solid-liquid-vapour) system in which bubble collapse takes place. In other words, in no instance where heaters are tested for hundreds of millions of cycles without a liquid present was surface damage similar to that reported in this section observed.

3.3. Cavitation versus chemical effects

Testing of several types of thin-film devices under more realistic, closed-pool conditions, namely with a nozzle in the close vicinity of the device, has yielded different results from those reported in Section 3.2. It has been noted in Table I that the device lifetime in closed-pool tests is significantly longer than the open-pool lifetime under similar drive conditions, as long as the drive voltage exceeds the minimum for generating a stable vapour blanket on top of the device and a stable jet stream through the nozzle [18]. Either lifetime can be fitted to an Arrhenius-type equation, which yields a significantly higher activation energy for the closed-pool runs.

From a microscopic point of view, inspection of all the closed-pool tested devices, whether open circuit or not, has not revealed the crater-like damage described in Section 3.2, which typifies devices tested under open-pool conditions. Thus Fig. 6a shows a typical damaged region of a device tested at 16 V (cf. 16.5 V required for nucleation/ejection) for 440 megacycles, in an open pool of pH 13 aqueous solution, whereas Fig. 6b shows the central region of a device tested at 24 V for 2 megacycles, in an open pool of pH 11 NaOH aqueous solution. Even though damages to the SiC:H overcoat film in these two devices may look similar at lower magnifications, they appear rather different at higher magnifications. In Fig. 6a, pits with rounded mouths are ubiquitous; the boundaries of these pits do not necessarily coincide with the grain boundaries observed in the amorphous film. These seem to suggest a chemical/electrochemical attack. Cavitation damage associated with bubble collapse is, obviously, absent in Fig. 6a, because the voltage has been too low for phase change to take place. Fig. 6b, on the other hand, shows typical cavitation-induced damage, as explained in Section 3.2.

The reduction of cavitation damage in the presence of a nearby nozzle plate is presumably attributable to variations in the transient, two-phase, three-dimensional, heat-transfer coupled fluid flow in the vicinity of the device surface. For example, the collapsing bubble, as observed by the strobed video-microphotography, appears to move away from the surface, contrary to other observations where the bubble tends to move toward a nearby solid surface during collapse [27]. Obviously, this must be due in part to the presence of the cone-shaped nozzle, which is only a few tens of micrometers away from the heater surface. The results of the parallel-plate experiments, shown in Fig. 7, are sufficient to show that local geometry and hydrodynamics do play a role in overcoat damaging. The solution used was a moderately corrosive ethylene glycol/water mixture, such that there is a non-trivial activation energy in the open-pool failure process. As the separation between the plate and the device narrows down, the average device lifetime increases accordingly. Since the devices are failed by a corrosion-dominating mechanism, several separations

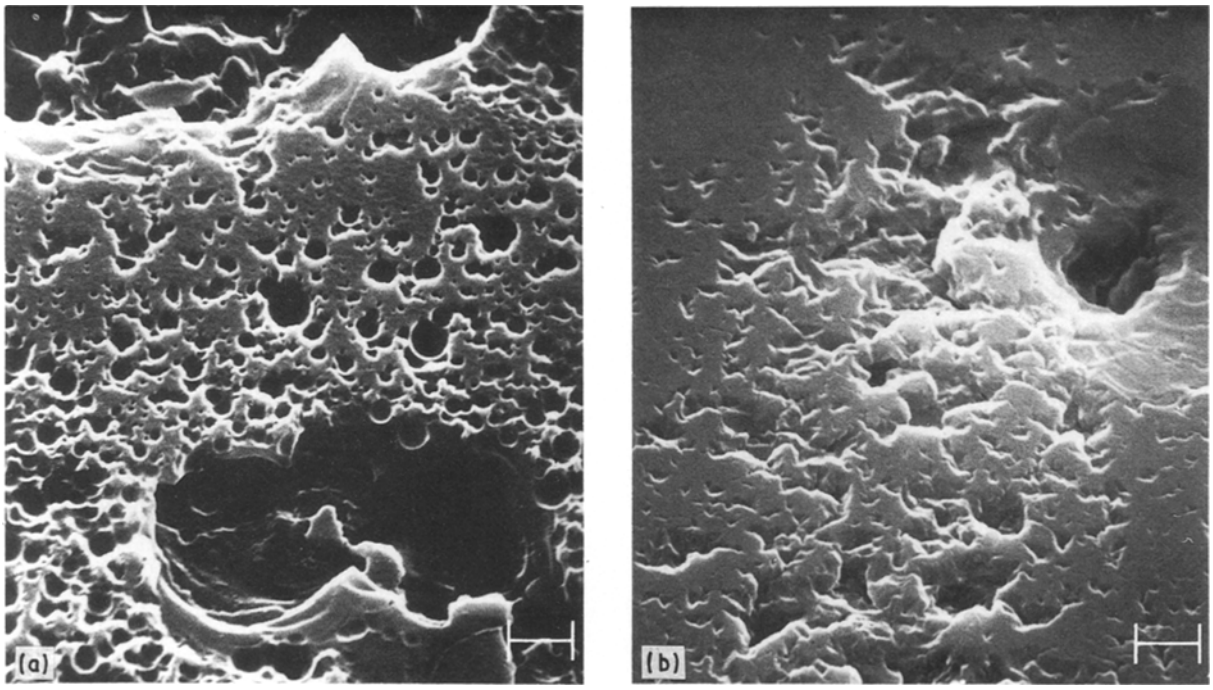

Figure 6 Scanning electron micrographs of two heaters showing (a) corrosion and (b) cavitation-induced damage. The length of the bar is 1 μm.

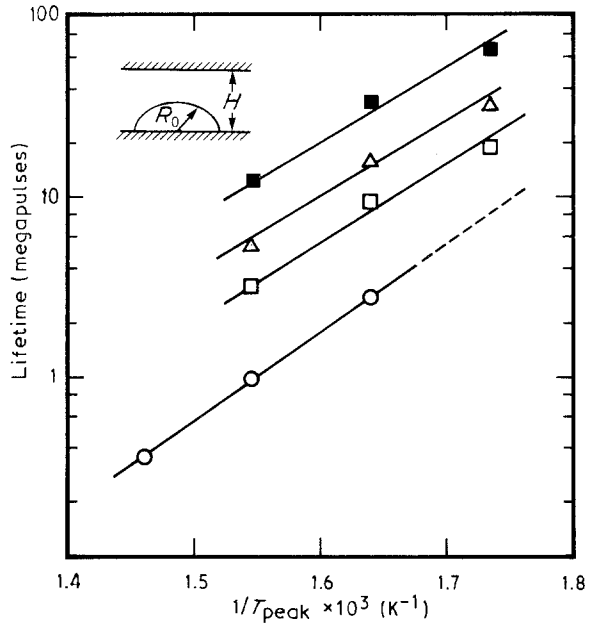

Figure 7 The effect of a parallel-plate on device lifetime as a function of the reciprocal peak surface temperature; (○) $H \rightarrow \infty$ (open-pool); (□) $H = 300$ μm; (△) $H = 150$ μm; (■) $H = 75$ μm.

give rise to a similar activation energy in each case. However, it is evident that the presence of a parallel plate reduces the contribution of hydrodynamics (cavitation) *vis-à-vis* that of corrosion.

3.4. Chemical etching of the α-SiC:H film

The thermal decomposition and subsequent deposition of chemical compounds over ink-jet heater surface, often called kogation [15], has an important effect on the integrity of the α-SiC:H film used as the topmost overcoat. In Fig. 8a, a device has become an open circuit because of a transverse crack initiated in the resistor layer. The latter was damaged because the protective carbide overcoat had been severely etched. As shown in Fig. 8b, both carbonaceous deposits (kogation) and etching of the SiC:H layer are evident on top of the device. The compositions of both regions of the surface have been corroborated by SAM.

Since virtually all dyes suitable for ink-jet printing have complex chemical structure, with azo bonds, functional groups (sulphonate, hydroxyl, carboxylate, to name a few), accompanying electrolytes, and impurities present, thermal decomposition and deposition processes of typical ink ingredients and the subsequent effects on α-SiC:H are extremely complicated. As a result, only the effects of pH as well as several salts and simple compounds are included in the present report. More importantly, the kinetics of typical etching effects is delineated with the data available.

Although one of the reasons for choosing the α-SiC:H film as the top passivation layer was its high chemical resistance, it is shown that under proper conditions it can be vigorously attacked. Thus, Fig. 9 shows the amount of etching of α-SiC:H plotted against test cycles for pH 8, 10, 11 and 12 solutions. The fact that a linear relationship is obtained in each case suggests there is little diffusion barrier effect for either reactants or products, and that the PECVD carbide is etched through a total dissolution process [28]. The effect of pH on α-SiC:H etching is also shown in Fig. 10, where the linear etch rate of α-SiC:H is plotted against the solution pH. The resulted curve bears strong resemblance to the curve obtained for α-SiO_2 dissolution in aqueous HCl and NaOH solution [29]. This suggests that etching of α-SiC:H films may incorporate dissolution of silicon oxide as an intermediate step. The surface of several heaters, including those which were unused, those used but not etched, and those severely etched, are examined by Auger depth profiling. It is found that all heaters examined

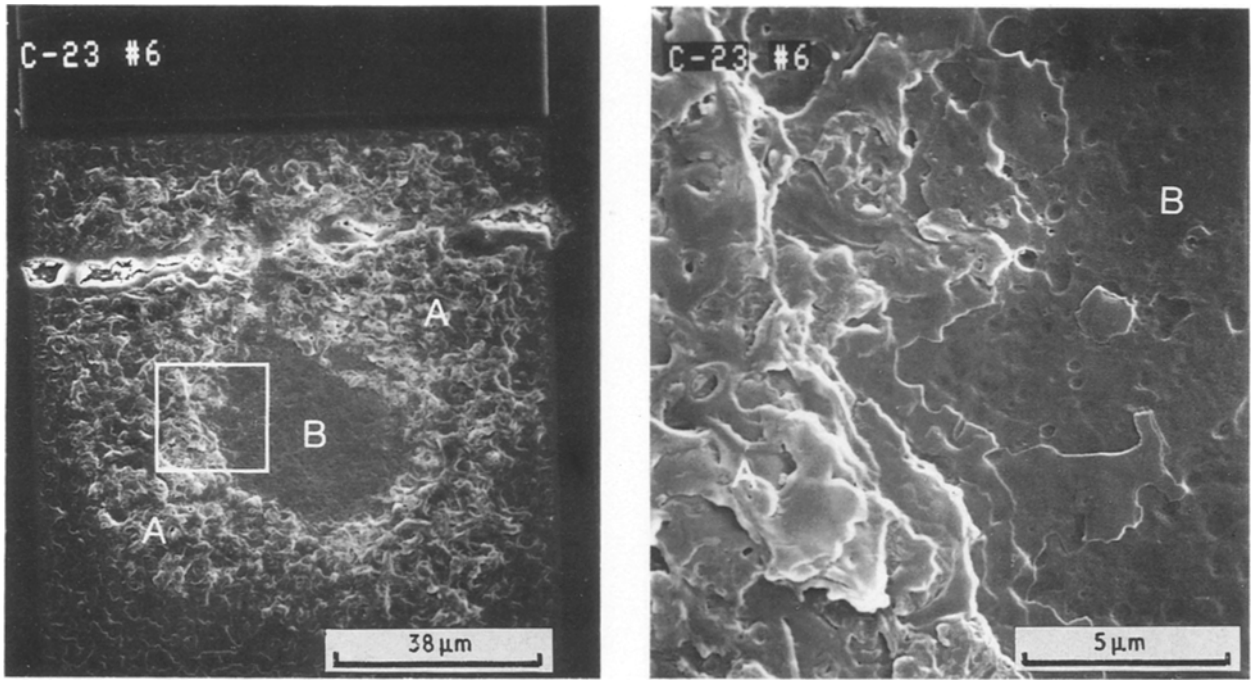

Figure 8 Kogation and etching of the α-SiC:H surface in a device tested in a typical ink. Regions A and B are kogation and etching, respectively.

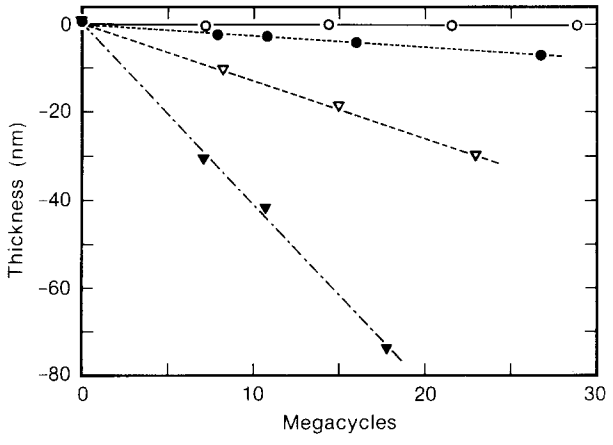

Figure 9 Reduction in α-SiC:H thickness as a function of test cycles for pH (○) 7.8, (●) 10, (▽) 11.4 and (▼) 12.1. Etching of carbide follows a linear kinetics in each case.

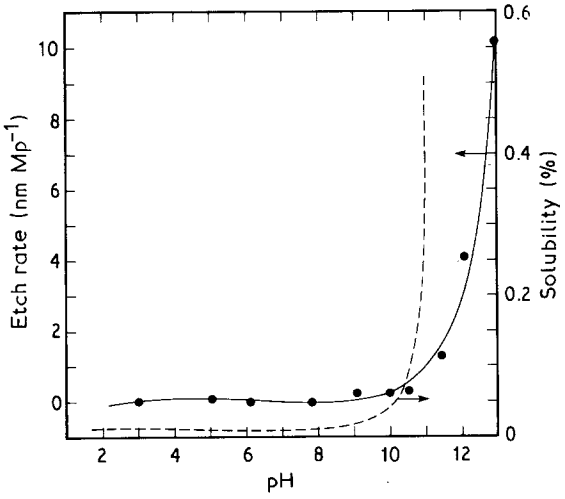

Figure 10 Linear etch rate of α-SiC:H as a function of solution pH (—●—). Also plotted is the solubility of α-SiO_2 in aqueous solutions (– – –) [28].

exhibit about the same Auger depth profile; to wit, there is a thin sub-oxide layer SiO_x at the top of the carbide layer, about 6–10 nm thick. The under-stoichiometric nature of surface oxide, manifested by the Si(O) LMM transition peak anywhere between 80 and 84 eV, instead of 76 eV, possibly refers to the presence of heterogeneous surface compositions and variations in bonding states (e.g. sp^3 versus sp^2) within the electron-beam-rastered area. Examples of several Auger surveys are given in Fig. 11. As the ion milling depth increases, there is a gradual shift of the Si(O) peak toward the metallic Si transition at 91 eV. The fact that all examined heaters show surface oxidation to the same degree, together with the above finding of linear kinetics, suggests the following mechanism for chemical etching of the α-SiC:H overcoat film under operating conditions pertinent to thermal ink-jet: (1) The thin SiO_x surface layer is dissolved in the test solution, which process may be accelerated by the presence of high pH or other chemicals; (2) the dissolved silicon or carbon species (silicates, CO, CO_2, etc.) are readily removed from the surface by the vigorous, recurring fluid motion associated with bubble growth and collapse, exposing a fresh α-SiC:H surface; (3) the surface is re-oxidized by vapour or other chemicals at high temperatures. Thus, it is the unique mechanism of effective removal of reaction products that contributes to both a linear etch rate and a thin surface oxide layer. A practical implication is that any chemical effect that enhances the rate process in either (1) or (3) above may be an etchant for the α-SiC:H film. A summary of etch rate for a number of simple salts and compounds is included as Table II; many such compounds are shown to generate either local alkalinity or radicals that vigorously attack and/or dissolve the material, and will be addressed separately [30].

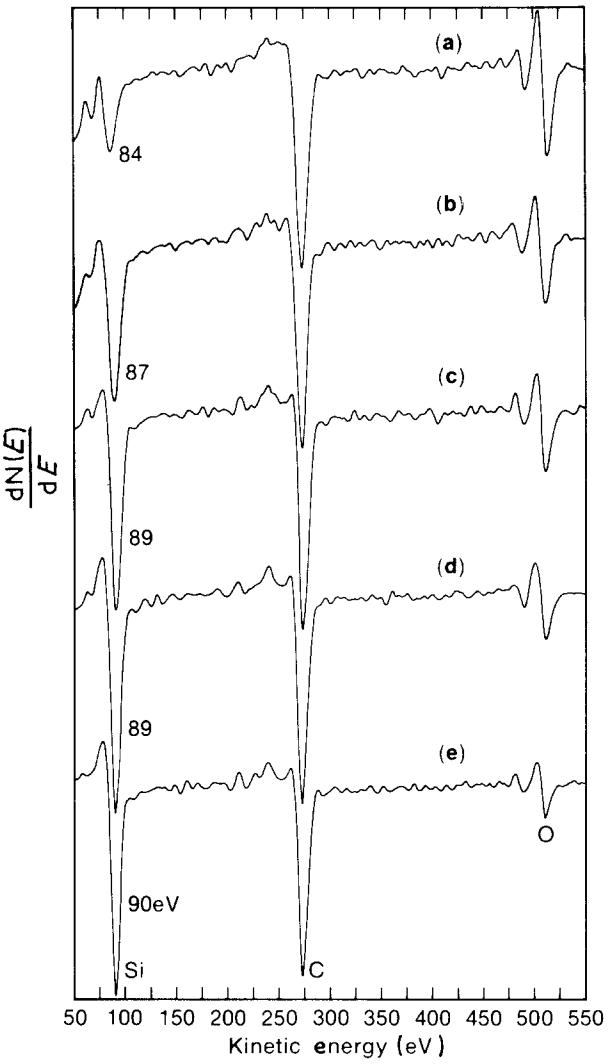

Figure 11 Auger surveys of the α-SiC:H overcoat film as a function of depth into the bulk of the film; (a) as-deposited surface; (b) 2 nm; (c) 4 nm; (d) 6 nm; and (e) 10 nm removed by argon ion milling.

TABLE II Etch rate of α-SiC:H by chemicals

Chemical	Concentration (w/w)	Etch rate (nm Mp^{-1})
NaCl	0.0016% (10 p.p.m. chloride)	0.025
NaCl	0.016% (100 p.p.m. chloride)	0.051
NaCl	0.16% (1000 p.p.m. chloride)	0.094
NaCl	1.6% (10000 p.p.m. chloride)	0.185
LiCl	0.012% (100 p.p.m. chloride)	0.0
LiCl	0.12% (1000 p.p.m. chloride)	0.072
LiCl	0.51% (4300 p.p.m. chloride)	0.24
NaBr	5%	0.10
NaI	5%	0.26
NaF	0.5%	1.8
NaH_2PO_4	5%	1.4
NaH_2BO_3	0.5%	1.6
Na_2SO_4	5%	0.51
Na_2SO_3	0.5%	0.24
$Na_2S_2O_5$	0.5%	0.090
H_2O_2	0.1%	0.38
H_2O_2	0.33%	1.25
NaN_3	1%	0.42

4. Conclusions

The breakdown of plasma-deposited, amorphous, hydrogenated silicon carbide films as a consequence of thermal, mechanical (hydrodynamic) and chemical stresses under operating conditions of a multilayer thin-film device is investigated. Specifically, the carbide-passivated device is driven by d.c. pulses of a few microseconds duration, at frequencies up to several kHz. The peak temperature during each cycle is normally well over 300 °C. Several failure modes of α-SiC:H have been identified; attempts have been made to elucidate the mechanisms involved in each.

Stress due to differential thermal expansion effects is shown to reach 1 GPa in the carbide layer when the device is heated under normal operating conditions. Thermal overload thus happens when the device is driven by pulses of excessive duration, amplitude or frequency, under which conditions, large thermal expansion mismatches result in delamination of the deposited layers from the substrate. Hydrogen evolution from the PECVD overcoat films as a result of elevated device temperature further accelerates the "pop-off" process, culminating in the catastrophic failure of the device. The device may also fail because of a thermal fatigue mechanism, especially when there are significant intrinsic stresses in the film or when the fluid media are corrosive. It is also noted that thin-film fracture or delamination may take place if the carbide layer is so thick as to store excessive elastic energy at the peak temperature.

Those devices which are tested in open pools of fluid and those which in enclosed space exhibit different failures and lifetime distributions. In the open-pool test, in which the device surface is exposed to a large pool of fluid, cavitation-induced damage to the carbide overcoat appears in the form of craters near the geometrical centre of the device, where the shock wave or microjet associated with bubble collapse is the highest. Such devices tend to fail rapidly. Alternatively, devices tested with an intact nozzle plate in place do not fail until the adverse effects of other influences (chemical as well as thermal) are established. Thus, although cavitation effects can not be totally excluded from the (closed-pool) ink-jet environment, it is mainly the chemical and thermal factors that contribute to overcoat and device failures under normal conditions. The exact role played by the nozzle plate in reducing cavitation damage is rather complicated; however, the simple geometrical effect of a parallel plate on device lifetime is shown to be in accordance with basic hydrodynamic principles.

Finally, chemical etching of the α-SiC:H layer is shown to be the main culprit causing device failure under most conditions. The thermal decomposition and deposition of insoluble debris over carbide surface is admittedly a complex phenomenon. However, by a "divide-and-attack" approach, effects of many inorganic and organic compounds on kogation and etching are studied. The mechanism of etching of α-SiC:H appears to consist of three recurring steps; the surface oxide is dissolved in the high-temperature environment; the dissolution products are readily moved away by the hydrodynamic agitation, exposing a fresh α-SiC:H surface; the surface is re-oxidized by vapour or chemicals in the high temperature environment. It is found that high pH solutions are especially

detrimental to α-SiC:H, removing the material at a linear etch rate in test cycles. Accordingly, it seems likely that thermo-chemical effects on the α-SiC:H thin film ultimately determine the integrity of a mechanically well-designed device.

References

1. W. E. NELSON, F. A. HALDEN and A. ROSENGREEN, *J. Appl. Phys.* **37** (1966) 333.
2. K. E. BEAN and P. S. GLEIN, *J. Electrochem. Soc.* **114** (1967) 1158.
3. K. KUROIWA and T. SUGANO, *ibid.* **120** (1973) 138.
4. A. J. LEARN and K. E. HAQ, *J. Appl. Phys.* **40** (1969) 430.
5. *Idem., Appl. Phys. Lett.* **17** (1970) 26.
6. D. A. ANDERSON and W. E. SPEAR, *Phil. Mag.* **35** (1977) 1.
7. Y. CATHERINE and G. TURBAN, *Thin Solid Films* **60** (1979) 193.
8. H. YOSHIHARA, H. MORI and M. KIUCHI, *ibid.* **76** (1981) 1.
9. D. ILIC, *Solid State Tech.* **25** (1982) 91.
10. A. SPROUL, D. R. McKENZIE and D. J. H. COCKAYNE, *Phil. Mag. B* **54** (1986) 113.
11. M. A. BAYNE, Z. KUROKAWA, N. U. OKORIE, B. D. ROE and L. JOHNSON, *Thin Solid Films* **107** (1983) 201.
12. K. KAMATA, N. AIZAWA and M. MORIYAMA, *J. Mater. Sci. Lett.* **5** (1986) 1055.
13. S. MOTOJIMA, N. IWAMORI, T. HATTORI and K. KUROSAWA, *J. Mater. Sci.* **21** (1986) 1363.
14. J. M. ELDRIDGE, J. O. MOORE, G. OLIVE and V. DUNTON, *J. Electrochem. Soc.* **137** (1990) 2266.
15. M. IKEDA, Presentation at the 18th Inst. Graphics Comm. Ann. Conf. on Ink-Jet Printing (Amsterdam, March, 1985).
16. E. V. BHASKAR and J. S. ADEN, *Hewlett-Packard J.* **36** (1985) 27.
17. G. OLIVE, J. M. ELDRIDGE and J. O. MOORE, Presentation at the 1986 Soc. Inform. Display (SID) Symposium (San Diego, May, 1986).
18. L. S. CHANG and G. OLIVE, *Proceedings SID* **28** (1987) 477.
19. L. S. CHANG, *ibid.* **30** (1989) 57.
20. W.-Y. LEE, *J. Appl. Phys.* **51** (1980) 3365.
21. M. A. PETRICH, K. K. GLEASON and J. A. REINER, *Phys. Rev. B* **36** (1987) 9722.
22. R. W. HOFFMAN, *Surf. Interf. Anal.* **3** (1981) 62.
23. J. H. JOU, L. HSU and L. S. CHANG, *Thin Solid Films* (in press).
24. E. KLOKHOLM, *IBM J. Res. Dev.* **31** (1987) 585.
25. E. SUHIR, ASME *J. Appl. Mech.* **53** (1986) 657.
26. A. KARIMI and J. L. MARTIN, *Int. Met. Rev.* **31** (1986) 1.
27. L. R. BLAKE, B. B. TAIB and G. DOHERTY, *J. Fluid Mech.* **170** (1988) 479.
28. L. S. CHANG and P. L. GENDLER, 63rd ACS Colloid and Surface Science Symposium (Seattle, June, 1989).
29. G. B. ALEXANDER, W. M. HESTON and R. K. ILER, *J. Phys. Chem.* **58** (1954) 453.
30. P. L. GENDLER and L. S. CHANG, submitted. *Chem. Mater.*

Received 27 November 1989
and accepted 18 June 1990